

See discussions, stats, and author profiles for this publication at: <https://www.researchgate.net/publication/26815636>

DFT Study on the Mechanisms of Stereoselective C(2)-Vinylation of 1-Substituted Imidazoles with 3-Phenyl-2-propynenitrile

ARTICLE in THE JOURNAL OF PHYSICAL CHEMISTRY A · SEPTEMBER 2009

Impact Factor: 2.69 · DOI: 10.1021/jp9047874 · Source: PubMed

CITATIONS

33

READS

21

2 AUTHORS:



Donghui Wei

Zhengzhou University

65 PUBLICATIONS 512 CITATIONS

SEE PROFILE



Mingsheng Tang

Zhengzhou University

95 PUBLICATIONS 1,385 CITATIONS

SEE PROFILE

Selective Decomposition of Alkyl Hydroperoxides on H-Type Zeolite via a Concerted Approach

Jinyun Yuan, Xincheng Liao, Hongming Wang,* Guanyu Yang,* and Mingsheng Tang

Center of Computational Chemistry, Department of Chemistry, Zhengzhou University, Zhengzhou, Henan, P. R. China

Received: September 5, 2008; Revised Manuscript Received: November 21, 2008

Catalyzed by H-type zeolite, the selective decomposition of alkyl hydroperoxides (HP), including 1-phenylethyl hydroperoxide (PEHP), phenylmethyl hydroperoxide (PMHP), and methyl hydroperoxide (MHP), to their corresponding carbonyl compounds and H₂O have been investigated by DFT calculations. In this calculation, a 19-atom cluster containing four tetrahedral atoms (denoted as **4T**) was used to model the H-type zeolite catalyst, and two competitive reaction channels were evaluated. Calculations predict that the concerted reaction channel is favorable for selective decomposition of alkyl hydroperoxides on the H-type zeolite from both kinetics and thermodynamics points of view. We found that the rate-determining step of the stepwise reaction channel proceeds via a one-hydrogen-bond transition state followed by dehydration. In the concerted reaction channel, whose transition state is an eight-membered ring with two hydrogen bonds, the decomposition of hydroperoxides occurs synchronously to form carbonyl compounds and H₂O, involving the proton exchange between hydroperoxides and the zeolite.

1. Introduction

Alkyl hydroperoxides have been extensively used as singlet oxygen donors in organic oxidations¹ and as initiator in free-radical polymerizations due to its relatively weak O–O linkage. On the other hand, alkyl hydroperoxides as the initial product of autooxidation often exist in the reaction mixture of industrial aerobic oxidation of hydrocarbons and also in the long-time-stored chemicals. However, due to their instability, alkyl hydroperoxides have caused many accidents so far, and they are designated as dangerous goods in regulations.² Furthermore, for industrial aerobic oxidation, alkyl hydroperoxides always can hardly be the target products, and they will decompose and react further to become more stable valuable products, such as ketone, alcohol, acid, etc. Unfortunately, such decomposition, especially under higher temperature, follows random free radical route to give the low selectivities of products. To improve the selectivity, one common method is the acid-catalyzed decomposition of alkyl hydroperoxides,³ which, however, is often not compatible with environmental, economical, and applicable demands due to the use of strong acids. Therefore, the research on selective decomposition of hydroperoxides is of important significance.⁴

Zeolites are crystalline aluminosilicates with oxygen-sharing silicate, [SiO₄]⁴⁻, and aluminate, [AlO₄]⁵⁻, tetrahedra. The presence of trivalent aluminum brings a negative charge within the crystal structure. In the H-type zeolites, H⁺ as counterion is mobile between the framework oxygens and responsible for its Brønsted acidity. Because of their acidity and porous nature, the H-type zeolites are widely used as heterogeneous acidic catalysts in various reactions, such as hydrocarbon cracking, alkylation, and isomerization, etc.,⁵ presenting the advantages of simple separability and recyclability.⁶ Recently, we have first found that the H-type zeolite can catalyze efficiently selective decomposition of 1-phenylethyl hydroperoxide (PEHP) to

acetophenone and H₂O under mild conditions.⁷ Obviously inconsistent with the random free radical mechanism or the acid-catalyzed decomposition, the hydroperoxide decomposition on the H-type zeolite, which is of significantly applicable potential, raises our attention.

A lot of theoretical researches on catalysis of the H-type zeolite for various reactions had been reported. Hydrogen exchange between water and various ZSM-5 zeolite surfaces was researched with first-principle density functional theory by Yang.⁸ Chan studied the design of effective zeolite catalysts for the complete hydrogenation of CO₂.⁹ Corma et al. examined the mechanism of the hydride transfer reaction between alkanes and alkenes catalyzed by an acidic zeolite.¹⁰ The mechanism of surface methoxy and dimethyl ether formation from methanol catalyzed by zeolitic protons was reported,¹¹ and also the reactivity of surface methoxy species in acidic zeolites was investigated in 2006 by Wang.¹² However, to the best of our knowledge, there is not any calculation investigation about hydroperoxide decomposition on zeolites.

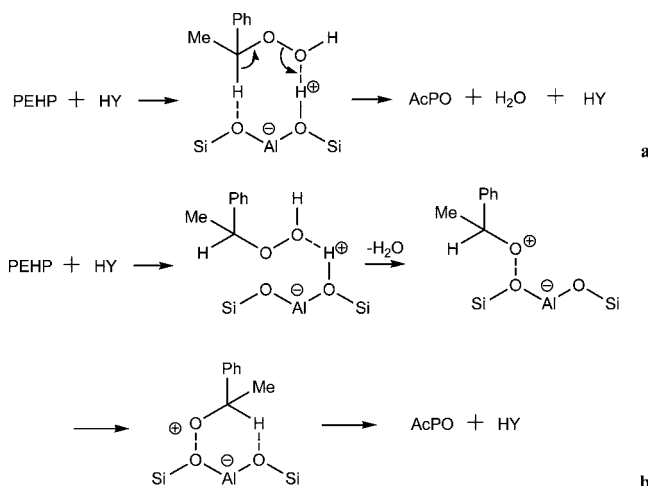
In our previous study of H-type zeolite catalyzing selective decomposition of PEHP, we found that the framework and the acidic proton of HY act together. A concerted mechanism, which forms an eight-membered ring transition state (Scheme 1a), was proposed, whereas another possible reaction channel, a stepwise one (Scheme 1b), maybe exists. Herein, these two competitive mechanisms will be investigated utilizing theoretical calculations, involving another two reactants, phenylmethyl hydroperoxide (PMHP) and methyl hydroperoxide (MHP), in order to understand this catalysis further.

2. Materials and Methods of Calculations

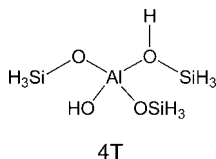
2.1. Experiment. 2.1.1. Preparation of the Zeolite HY. 20 g of zeolite NaY (Si/Al = 5.0) and 100 mL of aqueous solution of 1 mol/L NH₄Cl were stirred for 2 h at reflux conditions and then filtered. The obtained solid was treated with the same ionic exchange procedure for twice more. Afterward, the solid was

* Corresponding authors. E-mail: hmwang06@163.com, yangguanyu@zzu.edu.cn.

SCHEME 1: Suggested Ionic Mechanisms of Selective Decomposition of PEHP on the H-Type Zeolite: (a) Concerted Reaction Channel; (b) Stepwise Reaction Channel



SCHEME 2: 4T Cluster Model of the H-Type Zeolite^a



^a The "T" represents a Si or Al atom, and "4" is the total number of Si and Al atoms.

washed, filtered, dried at 100 °C, and then calcined under 400 °C for 5 h to give the zeolite HY.

2.1.2. Synthesis of PEHP. 0.1 mol of H₂SO₄ in 70% aqueous solution was dropped slowly into 0.1 mol of 1-phenylethanol under stirring at room temperature, and then 0.1 mol of H₂O₂ solution (90%) was added. After stirring for 7 h at room temperature and placed overnight, 20 mL of a saturated solution of NaCl was added into the reaction mixture under stirring. Then extraction using 3 × 10 mL of dichloromethane was operated. The dichloromethane layer was washed with saturated NaCl solution for three times, dried over anhydrous Na₂SO₄, and distilled under vacuum. The fraction of 60–70 °C was collected, which showed to be a mixture of 44.8% PEHP and 55.2% 1-phenylethanol on the basis of the GC analysis.

2.1.3. PEHP Decomposition by the Zeolite HY Catalysis. In 7 mL of acetonitrile, a 0.9127 g mixture of PEHP (44.8%) and 1-phenylethanol (55.2%), with 0.1517 g of zeolite HY, was stirred for 10 h at 80 °C under N₂. After being cooled to room temperature, the reaction solution was analyzed by GC. The results indicate that the reaction solution includes 8.7% PEHP, 36.1% acetophenone (AcPO), and 55.2% 1-phenylethanol, and the decomposition ratio of PEHP is 80.4%.

2.2. Method of Calculations. To explore the catalytic properties of the H-type zeolite from its local structure, a small 4T cluster including four tetrahedral atoms and totally 19 atoms as a model of the H-type zeolite (Scheme 2) was chosen. In this model, the dangling bonds were terminated with H atoms^{10–14} to satisfy the valencies, i.e., the cluster model was terminated with –SiH₃ linkages.¹⁵ To approximate the rigidity of the zeolite framework, the H atoms at the periphery of the cluster model are held fixed in space.^{13,16,17}

All calculations are performed with the density functional theory (DFT) using the hybrid B3LYP^{18–21} exchange-correlation

functional as implemented in the software package Gaussian03.²² Effective core potentials (ECP) are employed for Al and 6-31G(d,p) basis set for the other elements. In order to make sure that a basis set extension beyond 6-31G(d,p) would not seriously affect our results, further single-point energy calculations have been performed with the basis set 6-311+G(d,p) for the intermediates, transition states, and products of PEHP decomposition by 4T catalysis, and these results are consistent with those of the basis set 6-31G(d,p) (see Supporting Information). Vibration frequencies calculations were then performed at all of the optimized geometry structures. Each reactant, product, and intermediate has been confirmed to have no imaginary frequencies. The transition state has also been verified to have the unique imaginary frequency and indeed corresponds to the expected motion of atoms. Internal reaction coordinate (IRC) calculations following reaction paths in both directions from a given transition state were carried out in order to investigate the minimum connected by the transition state.

3. Results and Discussion

3.1. Experimental Section. In order to indicate that the H-type zeolite plays an important role when it catalyzed selectively PEHP decomposition to yield AcPO, we carried out the experiment of PEHP decomposition in the presence of the zeolite HY.⁷ Our experimental results show that 80.4% PEHP was converted into AcPO and H₂O. Our previous study on aerobic oxidation of ethylbenzene had proved that only introducing acidic condition without zeolite HY can not initiate this transform at the same conditions.⁷ On the other hand, it is known that through the free radical chain mechanism alkyl hydroperoxides decompose to its corresponding alcohol. Therefore, the H-type zeolite-catalyzed selective transformation of PEHP to AcPO cannot be explained by the free radical mechanism or the simple Brønsted acid catalysis mechanism.

3.2. Calculation Section. In the past decade, the cluster approach has been used by many theoretical studies to describe local phenomena of the zeolite-catalyzed reactions like the interaction of organic reactants with active sites on zeolites, bond breaking and bond formation processes, etc.,^{23–48} showing it provides a facile, efficient tool to simulate the catalytic active sites on zeolites.^{49,50} Among them, in consideration of the dominant interactions occurring between the reactants and the active sites as well as their neighbor atoms, the 4T cluster,^{51–54} a small cluster model, has been widely used to investigate the reaction on the active sites, although it should be recognized that the cage effect of zeolite ought to be addressed for the zeolite-catalyzed reactions. In fact, Chan and Radom's calculations indicate that the reaction trends obtained with the 4T clusters are consistent with those calculated with the larger 28T clusters, while the barriers are somewhat lower for the smaller system.⁹ Therefore, here the 4T cluster model (Scheme 2) was used to explore the catalytic properties of the H-type zeolite.

The PEHP decomposition over the H-type zeolite through the two reaction channels was calculated with the 4T cluster model. The optimized structures of three transition states of the hydroperoxide at the surface of the H-type zeolite (TSs) are shown in Figure 1, and the reaction energy profiles are shown in Figure 2. No matter what is the concerted or the stepwise reaction channel, hydroperoxide moves to the active sites of the H-type zeolite to form the intermediate and then form the transition state through hydrogen bonds interaction. The main discrepancy is that there are different hydrogen bonds in the stepwise and the concerted transition states. In the concerted reaction channel, via the intermediate (IN), the

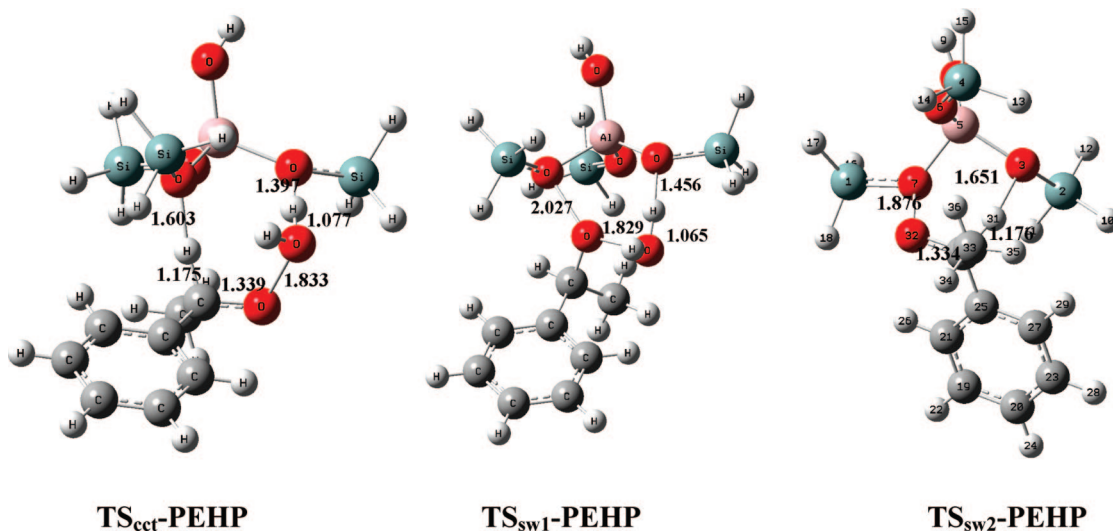


Figure 1. Optimized structures of TS_{cct} , TS_{sw1} , and TS_{sw2} for PEHP (bond lengths are in angstroms).

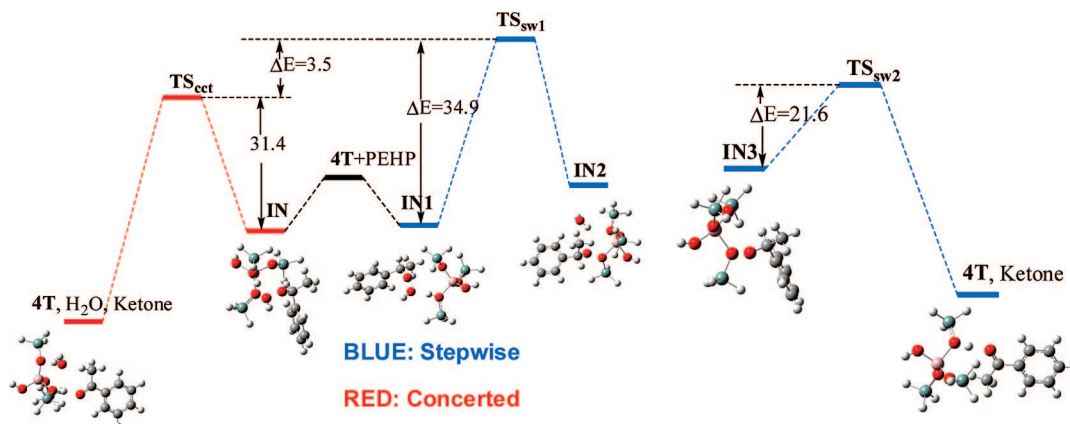


Figure 2. Reaction energy profile for H-type zeolite-catalyzed PEHP decomposition channels (kcal/mol).

transition state of hydroperoxide at the surface of the H-type zeolite (TS_{cct}) is formed which has an eight-membered ring and two hydrogen bonds of $\text{O}-\text{H}\cdots\text{O}$ and $\text{C}-\text{H}\cdots\text{O}$ (see Figure 1). In the beginning of the stepwise reaction channel, the intermediate (IN1) converts into the transition state (TS_{sw1}) with one hydrogen bond of $\text{O}-\text{H}\cdots\text{O}$. Next, the TS_{sw1} transforms to the intermediate (IN2) which includes a H_2O molecule. Finally, the intermediate (IN3), the dehydrated fragment of TS_{sw1} , passes the transition state (TS_{sw2}) into ketone or aldehyde (see Figure 2). In comparison with the bonding lengths of the sole PEHP and 4T , it has been observed that the bonds of $\text{O}-\text{O}$ and $\text{C}-\text{H}$ are elongated by about 0.375 and 0.076 Å in $\text{TS}_{\text{cct}}\text{-PEHP}$, respectively, and the $\text{C}-\text{O}$ bond of PEHP is shortened by 0.102 Å, while the $\text{O}-\text{H}$ bond of 4T is elongated by 0.426 Å. Such changes of the bonds and the atomic motion in the imaginary frequency show a synchronous reaction tendency: (1) the cleavage of $\text{O}-\text{O}$ and $\text{C}-\text{H}$ bonds of PEHP, (2) a H_2O molecule production via a new $\text{O}-\text{H}$ bond formation between the hydroxyl of PEHP and the proton of 4T , (3) the contraction of $\text{C}-\text{O}$ bond of PEHP to give carbonyl, and (4) another new $\text{O}-\text{H}$ formation to resume the catalyst 4T , which involves the proton exchange.

In $\text{TS}_{\text{sw1}}\text{-PEHP}$, the first TS of PEHP decomposition in the stepwise mechanism, $\text{O}-\text{H}$ of 4T is elongated by 0.485 Å and the $\text{O}-\text{O}$ of PEHP is elongated by 0.371 Å, implying the cleavages of $\text{O}-\text{O}$ of PEHP and $\text{O}-\text{H}$ of 4T . As a result, the 4T donated a proton and PEHP donated a hydroxyl ion to form

a H_2O molecule. The fragment of PEHP is adsorbed to the deprotonated H-type zeolite 4T by $\text{O}-\text{O}$ interaction and then form the second TS, $\text{TS}_{\text{sw2}}\text{-PEHP}$, which has a six-membered ring structure. The calculations indicate that in $\text{TS}_{\text{sw2}}\text{-PEHP}$ the $\text{C}-\text{O}$ bond of PEHP is shortened by 0.122 Å, the $\text{C}-\text{H}$ bond of PEHP and $\text{O}-\text{O}$ bond between PEHP and 4T are elongated by 0.083 and 0.398 Å relative to its intermediate (IN3), showing a tendency of the contraction of PEHP $\text{C}-\text{O}$ bond to give a carbonyl and a new $\text{O}-\text{H}$ formation to resume the catalyst 4T .

As seen in Figure 2, in the stepwise reaction channel, the calculated activation energy of the transformation from IN1 to IN2 via TS_{sw1} (the first step) is 34.9 kcal/mol, higher than that of the second step (21.6 kcal/mol). This suggests that the first step is the rate-determining step of the stepwise reaction channel. Besides, calculations show that the energy of IN2 is 7.9 kcal/mol higher than that of IN1 , implying this step is endothermic. Comparatively, the activation energy of the concerted transition state ($\text{TS}_{\text{cct}}\text{-PEHP}$) is 31.4 kcal/mol, lower than that of the rate-determining step in the stepwise reaction channel. Moreover, the product of the concerted reaction channel is 73.2 kcal/mol below IN , indicating the concerted reaction channel is exothermic. As a result, though the difference of only 3.5 kcal/mol between the two activation barriers of the concerted reaction channel and the rate-determining step in the stepwise reaction channel could not affirm which is the exclusive one, PEHP decomposition by the H-type zeolite catalyst through the concerted reaction channel is favorable as viewed from both kinetics and thermodynamics.

TABLE 1: Activation Energies and Changes of Bond Lengths of Various Hydroperoxides and 4T^a

	TS _{cct}					TS _{sw1}				TS _{sw2}		
	<i>E</i>	bond change (Å)				<i>E</i>	bond change (Å)		<i>E</i>	bond change (Å)		
		O–O ^b	O–H ^c	C–O ^b	C–H ^b		O–O ^b	O–H ^c		C–H ^b	C–O ^b	O–O ^d
PEHP	31.4	+0.375	+0.426	−0.102	+0.076	34.9	+0.371	+0.485	21.6	+0.083	−0.122	+0.398
PMHP	30.5	+0.356	+0.385	−0.122	+0.077	37.2	+0.352	+0.478	19.9	+0.090	−0.116	+0.373
MHP	30.7	+0.366	+0.483	−0.088	+0.118	41.2	+0.345	+0.427	23.0	+0.116	−0.102	+0.384

^a *E* is the activation energy (kcal/mol); the bond changes (Å) are in comparison with those of the sole hydroperoxides, 4T and their IN3s.

^b The bonds of hydroperoxides. ^c The bonds of 4T. ^d The bonds between hydroperoxides and 4T; “+” and “−” mean elongation and shortening of bond, respectively.

The H-type zeolite-catalyzed decompositions of the other two hydroperoxides, PMHP and MHP, were also investigated with the same theory method. The bond changes and the activation energies of all TSs in both the concerted reaction channel and the stepwise reaction channel are displayed in Table 1. Whichever reaction channel they take, the bond changes and reaction tendencies in decompositions of both PMHP and MHP are similar to those of PEHP. In TS_{cct}s, the O—O and C—H bonds of hydroperoxides and the O—H bond of 4T are elongated; the C—O bonds of the hydroperoxides are shortened. In TS_{sw1}s, the O—H of 4T and the O—O of hydroperoxides are elongated, the C—O bond of hydroperoxides is shortened, and the C—H bond of hydroperoxides and the O—O bond between hydroperoxides and 4T are elongated in TS_{sw2}s as well. All the bond changes imply the same reaction tendency of the H-type zeolite-catalyzed decomposition of hydroperoxides to corresponding carbonyl compounds and H₂O. And again, the calculated results of the activation barriers show that the first step is the rate-determining step of the stepwise reaction channel for both PMHP and MHP. However, between the two reaction channels, the activation barrier differences of PMHP and MHP are 6.7 and 10.5 kcal/mol, respectively. These barrier differences are higher than that of PEHP (3.5 kcal/mol), probably since the lower steric influences of PMHP and MHP result in that the transition state TS_{cct}-PMHP and TS_{cct}-MHP in the concerted reaction channel are formed more easily. In addition, the concerted reaction channel products of PMHP and MHP are 71.2 and 53.8 kcal/mol below their INs, respectively, meaning that they are exothermic. Nevertheless, for their rate-determining step of the stepwise reaction channels, they are endothermic because their products are 10.3 and 14.8 kcal/mol higher than their IN1s. Consequently, for PMHP and MHP, the concerted reaction channel is also favorable kinetically and thermodynamically.

4. Conclusions

The decomposition of 1-phenylethyl hydroperoxide (PEHP) to acetophenone and H₂O catalyzed by zeolite HY was found experimentally. The selective decomposition of PEHP has also been explored theoretically using DFT calculations, where a 19-atom cluster containing four tetrahedral atoms (denoted 4T) was used to model the H-type zeolite catalyst. The theoretical studies were extended to phenylmethyl hydroperoxide (PMHP) and methyl hydroperoxide (MHP) decomposition. Two competitive reaction channels, a concerted reaction channel via an eight-membered-ring TS with two hydrogen bonds and a stepwise reaction channel via one-hydrogen-bond TS in each step, have been evaluated. The calculations demonstrate that both reaction channels lead to the decomposition of hydroperoxides to their corresponding carbonyl compounds and H₂O. However, the concerted reaction channel has a lower activation barrier than the rate-determining step of the stepwise reaction

channel. As a consequence, as viewed from both kinetics and thermodynamics, the concerted reaction channel is favorable for selective decomposition of alkyl hydroperoxides on the H-type zeolite.

Acknowledgment. This work was supported by the National Natural Science Foundation of China (Grant No. 20672104).

Supporting Information Available: Cartesian atomic coordinates of the structures of all TSs and the single-point energies of the intermediates, transition states, and products of PEHP decomposition obtained using 6-31G(d,p) and 6-311+G(d,p) basis sets. This material is available free of charge via the Internet at <http://pubs.acs.org>.

References and Notes

- (1) Gelalcha, F. G. *Chem. Rev.* **2007**, *107*, 3338.
- (2) (a) Malow, M.; Wehrstedt, K. D. *J. Hazard Mater.* **2005**, *120*, 21. (b) Miyake, A.; Yamada, N.; Ogawa, T. *J. Loss Prevent. Proc.* **2005**, *18*, 380.
- (3) (a) Schmidt, R. J. *Appl. Catal. A: Gen.* **2005**, *280*, 89. (b) Sun, Z.; Xu, J.; Du, Z.; Zhang, W. *Appl. Catal. A: Gen.* **2007**, *323*, 119.
- (4) Yadav, G. D.; Asthana, N. S. *Appl. Catal. A: Gen.* **2003**, *244*, 341.
- (5) Ryder, J. A.; Chakraborty, A. K.; Bell, A. T. *J. Phys. Chem. B* **2000**, *104*, 6998.
- (6) Venuto, P. B. *Microporous Mater.* **1997**, *2*, 297.
- (7) Yang, G.; Ma, Y.; Xu, J. *J. Am. Chem. Soc.* **2004**, *126*, 10542.
- (8) Yang, G.; Liu, X.; Han, X.; Bao, X. *J. Phys. Chem. B* **2006**, *110*, 23388.
- (9) Chan, B.; Radom, L. *J. Am. Chem. Soc.* **2006**, *128*, 5323.
- (10) Boronat, M.; Viruela, P.; Corma, A. *J. Phys. Chem. A* **1998**, *102*, 9863.
- (11) Blaszkowski, S. R.; van Santen, R. A. *J. Phys. Chem. B* **1997**, *101*, 2292.
- (12) Jiang, Y.; Hunger, M.; Wang, W. *J. Am. Chem. Soc.* **2006**, *128*, 11679.
- (13) David, H.; Wells, J.; Joshi, A. M.; Nicholas, D. W.; Thomson, K. T. *J. Phys. Chem. B* **2006**, *110*, 14627.
- (14) Boronat, M.; Viruela, P. M.; Corma, A. *J. Am. Chem. Soc.* **2004**, *126*, 3300.
- (15) Arstad, B.; Nicholas, J. B.; Haw, J. F. *J. Am. Chem. Soc.* **2004**, *126*, 2991.
- (16) Fermann, J. T.; Auerbach, S. M. *J. Phys. Chem. A* **2001**, *105*, 2879.
- (17) Kassab, E.; Jessri, H.; Allavena, M.; White, D. *J. Phys. Chem. A* **1999**, *103*, 2766.
- (18) Becke, A. D. *Phys. Rev. A* **1998**, *38*, 3098.
- (19) Becke, A. D. *J. Chem. Phys.* **1993**, *98*, 5648.
- (20) Lee, C.; Yang, W.; Parr, R. G. *Phys. Rev. B* **1998**, *37*, 785.
- (21) Stephens, P. J.; Devlin, F. J.; Chabalowski, C. F.; Frisch, M. J. *J. Phys. Chem.* **1994**, *98*, 11623.
- (22) Frisch, M. J.; et al. *Gaussian 03, revision C.02*; Gaussian, Inc.: Wallingford, CT, 2004 (SN: PC21390756W-4203N).
- (23) Boronat, M.; Claudio, M.; Wilson, Z.; Viruela, P.; Corma, A. *J. Phys. Chem. B* **2001**, *105*, 11169.
- (24) Van Santen, R. A. *Catal. Today* **1997**, *38*, 157.
- (25) Redondo, A.; Hay, P. J. *J. Phys. Chem.* **1993**, *97*, 11754.
- (26) Sauer, J.; Kolmel, C. M.; Hill, J. R.; Ahlrichs, R. *Chem. Phys. Lett.* **1989**, *164*, 193.
- (27) Sauer, J. In *Modeling of Structure and Reactivity in Zeolites*; Catlow, C. R. A., Ed.; Academic Press: San Diego, CA, 1992.

- (28) Sauer, J.; Sierka, M.; Haase, F. In *Transition State Modeling for Catalysis*; ACS Symposium Series 721; Truhlar, D. G., Morokuma, K., Eds.; American Chemical Society: Washington, DC, 1999; p 359.
- (29) Zygmunt, S. A.; Mueller, R. M.; Curtiss, L. A.; Iton, L. E. *J. Mol. Struct.* **1998**, *430*, 9.
- (30) Gonzales, N. O.; Bell, A. T.; Chakraborty, A. K. *J. Phys. Chem. B* **1997**, *101*, 10058.
- (31) Rice, M. J.; Chakraborty, A. K.; Bell, A. T. *J. Phys. Chem. B* **1998**, *102*, 7498.
- (32) Gale, J. D. *Top. Catal.* **1996**, *3*, 169.
- (33) Greatbanks, S. P.; Hillier, I. H.; Burton, N. A. *J. Chem. Phys.* **1996**, *105*, 3770.
- (34) Zygmunt, S. A.; Curtiss, L. A.; Iton, L. E.; Erhardt, M. K. *J. Phys. Chem.* **1996**, *100*, 6663.
- (35) Krossner, M.; Sauer, J. *J. Phys. Chem.* **1996**, *100*, 6199.
- (36) Jobic, H.; Tuel, A.; Krossner, M.; Sauer, J. *J. Phys. Chem.* **1996**, *100*, 19545.
- (37) Gale, J. D.; Catlow, C. R. A.; Carruthers, J. R. *Chem. Phys. Lett.* **1993**, *216*, 155.
- (38) Blaszkowski, S. R.; van Santen, R. A. *J. Phys. Chem.* **1995**, *99*, 11728.
- (39) Bates, S.; Dwyer, J. *J. Mol. Struct.* **1994**, *112*, 57.
- (40) Haase, F.; Sauer, J. *J. Am. Chem. Soc.* **1995**, *117*, 3780.
- (41) Allavena, M.; Kassab, E.; Evleth, E. *J. Mol. Struct.* **1994**, *325*, 85.
- (42) Evleth, E. M.; Kassab, E.; Sierra, L. R. *J. Phys. Chem.* **1994**, *98*, 1421.
- (43) Blaszkowski, S. R.; Nascimento, M. A. C.; van Santen, R. A. *J. Phys. Chem.* **1996**, *100*, 3463.
- (44) Blaszkowski, S. R.; Jansen, A. P. J.; Nascimento, M. A. C.; van Santen, R. A. *J. Phys. Chem.* **1994**, *98*, 12938.
- (45) Kramer, G. J.; van Santen, R. A. *J. Am. Chem. Soc.* **1995**, *117*, 1766.
- (46) Truong, T. N. *J. Phys. Chem. B* **1997**, *101*, 2750.
- (47) Esteves, P. M.; Nascimento, A. C.; Mota, J. A. *J. Phys. Chem. B* **1999**, *103*, 10417.
- (48) Beck, L. W.; Xu, T.; Nicholas, J. B.; Haw, J. F. *J. Am. Chem. Soc.* **1995**, *117*, 11594.
- (49) Sremaniak, L. S.; Whitten, J. L.; Truitt, M. J.; White, J. L. *J. Phys. Chem. B* **2006**, *110*, 20762.
- (50) (a) Kramer, G. J.; de Man, A. J. M.; van Santen, R. A. *J. Am. Chem. Soc.* **1991**, *113*, 6435. (b) Frash, M. V.; van Santen, R. A. *Top. Catal.* **1999**, *9*, 191.
- (51) Arstad, B.; Kolboe, S.; Swang, O. *J. Phys. Chem. B* **2002**, *106*, 12722.
- (52) Svelle, S.; Kolboe, S.; Swang, O. *J. Phys. Chem. B* **2004**, *108*, 2953.
- (53) Vos, A. M.; Schoonheydt, R. A.; Proft, F. D.; Geerlings, P. *J. Phys. Chem. B* **2003**, *107*, 2001.
- (54) Vos, A. M.; Rozanska, X.; Schoonheydt, R. A.; van Santen, R. A.; Hutschka, F.; Hafner, J. *J. Am. Chem. Soc.* **2001**, *123*, 2799.

JP8079167